Article type: Regular paper

Overexpression, Characterization and Crystallization of the Functional Domain of Cytochrome c_z from *Chlorobium tepidum*

Makoto Higuchi[1], Yu Hirano[1, 2], Yukihiro Kimura[3], Hirozo Oh-oka[4], Kunio Miki[2] & Zheng-Yu Wang[1,*]

[1] *Faculty of Science, Ibaraki University, Mito 310-8512, Japan*

[2] *Department of Chemistry, Graduate School of Science, Kyoto University, Sakyo-ku, Kyoto 606-8502, Japan*

[3] *Organization of Advanced Science and Technology, Kobe University, 1-1 Rokkodai, Nada, Kobe 657-8501, Japan*

[4] *Department of Biological Sciences, Graduate School of Science, Osaka University, Toyonaka, Osaka 560-0043, Japan*

* *Author for correspondence (e-mail: wang@mx.ibaraki.ac.jp; fax: +81-29-228-8352)*

Keywords: green sulfur bacteria; reaction center; electron transfer; heme protein

ABSTRACT

Cytochrome c_z is found in green sulfur photosynthetic bacteria and is considered to be the only electron donor to the special pair P840 of the reaction center. It consists of a N-terminal transmembrane domain and a C-terminal soluble domain that binds a single heme group. Large scale expression of the C-terminal functional domain of the cytochrome c_z (C-cyt c_z) from the thermophilic bacterium *Chlorobium tepidum* has been achieved using the *Escherichia coli* expression system. The C-cyt c_z expressed has been highly purified and is stable at room temperature over 10 days of incubation for both reduced and oxidized forms. Spectroscopic measurements indicate that the heme iron in C-cyt c_z is in a low-spin state and this does not change with the redox state. ^{1}H-NMR spectra of the oxidized C-cyt c_z exhibited unusually large paramagnetic chemical shifts for the heme methyl protons in comparison with those of other Class I ferric cytochromes *c*. Differences in the ^{1}H-NMR linewidth were observed for some resonances, indicating different dynamic environments for these protons. Crystals of the oxidized C-cyt c_z were obtained using ammonium sulfate as a precipitant. The crystals diffracted X-rays to a maximum resolution of 1.2 Å, and the diffraction data were collected to 1.3 Å resolution.

Abbreviations: C-cyt c_z, C-terminal domain of the cytochrome c_z; *Chl, Chlorobium*; CD, circular dichroism; MALDI-TOF, matrix-assisted laser desorption/ionization time-of-flight; MCD, magnetic circular dichroism; PCR, polymerase chain reaction; PEG, polyethylene glycol; RC, reaction center; RR, resonance Raman

Introduction

The green sulfur bacterial reaction center (RC) shares many similarities to those of heliobacteria and Photosystem I of higher plants. These include the presence of the same set of electron acceptors and a similar polypeptide composition of core and F_A/F_B proteins (Feiler and Hauska, 1995; Oh-oka, 2007). They are also similar to the purple bacterial-type RC in the way that a bacteriochlorophyll *a* dimer (P840) serves as the primary donor and there is a RC-associated cytochrome as electron donor to the photo-oxidized P840. In the *Chlorobiaceae* species, the RC-associated cytochrome (cyt) with a molecular mass of about 23 kDa is a *c*-type membrane-bound monoheme protein that copurifies with the RC and has an α-band absorbing at 551-552 nm in reduced form (Hurt and Hauska, 1984; Oh-oka et al., 1995; Okumura et al., 1994). Its unusual primary structure suggests three transmembrane helices at the N-terminus and has the heme-binding moiety close to the C-terminus (Okkels et al., 1992). Due to the low sequence similarity around the heme-binding site and the unique position of the binding site compared with other *c*-type heme proteins, the cyt *c* is classified as a novel class of membrane-bound cyt protein (Okkels et al., 1992) and has been designated as cyt c_z (Oh-oka et al., 1998).

The cyt c_z appears to have two copies per RC in both membrane preparation (Okumura et al., 1994) and isolated RC complex (Oh-oka et al., 1995). It functions as immediate electron donor to P840 with a midpoint potential of 180 mV (Okumura et al., 1994), about 50 mV more negative than the P840 (Kusumoto et al., 1999). The period of electron transfer from cyt c_z to P840 is 7 μs in whole cells, and ~100 μs in isolated RCs

(Hauska et al., 2001). Strong viscosity dependence of the rate constant was observed for the isolated RC complex from *Chlorobium*(*Chl.*) *tepidum*, indicating a conformational fluctuation of the heme-containing moiety of cyt c_z in the suspending medium (Oh-oka et al., 1997). This is consistent with the topological arrangement of cyt c_z where its N-terminal domain is assumed to be anchored in the lipid membrane and the hydrophilic heme-binding domain serves as a flexible shuttle to mediate electron transfer to P840. Recently, the electron donors to the photo-oxidized cyt c_z have been identified. The study shows that the cyt c_z can be rapidly reduced by a parallel electron donation pathway from a soluble cyt c_{554} and the membrane-bound menaquinol:cyt *c* oxidoreductase (Tsukatani et al., 2008). The reduction rates from both routes are almost the same under the in vitro experimental condition, and the two pathways seem to function independently.

Despite the long history of research on the cyt c_z, structural investigation has been largely delayed. To our knowledge, no high-resolution structure has been available for the membrane-bound *c*-type heme proteins, including the purple bacterial counterpart cyt c_y (Jenney et al., 1994; Lee et al., 2008). This situation may be attributed to the small amount of the proteins in native cells and the difficulties in purification due to the hydrophobic nature of membrane protein. Towards structure determination and understanding of molecular mechanism of the electron transfer of cyt c_z, we developed a system in this study to overexpress the C-terminal functional domain of the cyt c_z (C-cyt c_z) from *Chl. tepidum* in *Escherichia* (*E.*) *coli* cells. Detailed characterization of the product has been described and shows that the C-cyt c_z expressed is fully functional. The

C-cyt c_z has been crystallized, and results of the structural analysis will be described elsewhere (Hirano et al., 2009).

Materials and methods

Construction of the C-cyt c_z *Expression Plasmid.* The procedure used to construct the C-cyt c_z plasmid was similar to that reported elsewhere (Onodera et al., 2007). A fragment from 351 bp to 618 bp in the *pscC* gene coding for the functional moiety of *Chl. tepidum* cyt c_z from Ala117 to Phe206 was amplified by PCR using the following primer pairs: (forward) 5'-GCGGCCATGGCTGAACTCAAAGAGTTC-3' and (reverse) 5'-GCGGGATCCTCAGAACTTCTCGTGGAGCCAG -3' (restriction sites underlined) according to the published sequence of the *pscC* gene (Oh-oka et al., 1997; Oh-oka et al., 2002). The primers corresponding to the 5' ends were designed to introduce a *Nco*I site in the forward primer and a *Bam*HI site in the reverse primer, respectively. The PCR fragment was digested with *Nco*I/*Bam*HI restriction enzymes (TaKaRa Bio Inc., Japan) and inserted into the multiple cloning site of expression vector pET-20b(+) (Novagen Inc., Madison, WI, USA) which carries an N-terminal *pelB* signal sequence for potential periplasmic localization of the target proteins. The cloning result was confirmed by nucleotide sequencing of the entire coding regions.

Overexpression and Purification of the C-cyt c_z. For expression, the constructed plasmid

was cotransformed with pEC86 plasmid (a generous gift from Dr. L. Thöny-Meyer) (Arslan et al., 1998) into *E. coli* C41(DE3) (Miroux and Walker, 1996). A 10 mL Terrific broth culture supplemented with 60 μg/mL ampicillin and 37 μg/mL chloramphenicol was grown at 37˚C for 7 h. The pre-culture was used as an inoculum for a 250 mL fermentation in Terrific broth supplemented with 70 μg/mL ampicillin and 37 μg/mL chloramphenicol. Cells were grown at 30˚C for 60 h and harvested by centrifugation (10000g) at 4˚C for 10 min. The C-cyt c_z was extracted by osmotic shock following the procedure described in the Novagen pET System Manual (11th Edition). The supernatant was concentrated (Amicon, YM-10) and then loaded onto a DEAE column (Toyopearl 650S, TOSOH) equilibrated at 10 ˚C with 30 mM Tris-HCl buffer (pH 8.5). The eluted C-cyt c_z was further purified by size-exclusion chromatography (Sephadex G-100 Superfine, Pharmacia) equilibrated at 10 ˚C with 30 mM Tris-HCl buffer (pH 8.5). The fractions with ratios of $A_{410}/A_{280} > 6.0$ in oxidized form were collected for the characterization and crystallization experiments.

Characterization of the Expressed C-cyt c_z. SDS-PAGE was performed using a modified tricine gel system for peptides as described (Judd, 2002). Peptide molecular weight marker "DAIICHI" (Daiichi Pure Chemicals Co. Ltd., Japan) was employed. Mass measurement was performed using MALDI-TOF/MS (AUTOFLEX, Bruker Daltonics, Germany) with the same method as given elsewhere (Onodera et al., 2007). Absorption spectra were measured using a Beckman DU-640 spectrophotometer with a wavelength range from 250

nm to 750 nm. The reduced form was prepared by addition of dithiothreitol to a final concentration of 1 mM. Both CD and MCD spectra were recorded at room temperature on a Jasco J-720w spectropolarimeter as described elsewhere (Suzuki et al., 2007). For CD measurement, the wavelength range was from 200 nm to 600 nm, scan speed 20 nm/min, band width 1.0 nm and the response 1 s. For MCD measurement, an electromagnet was used to produce an external magnetic field of 1.5 T. The wavelength range was from 250 nm to 600 nm, scan speed 50 nm/min, band width 0.5 nm and the response 1 s. Final MCD spectra were obtained by subtracting the negative signals from the positive ones and therefore corresponded to those obtained under a magnetic field of 3.0 T.

^{1}H-NMR spectra were collected on a Bruker AVANCE DRX-400 spectrometer equipped with a variable-temperature controller. A 5-mm TXI triple-resonance inverse probe with z-axis field gradient was used. One dimensional ^{1}H spectra were recorded with 16K data points, acquisition time of 0.215 s, and 600 accumulations. C-cyt c_z was concentrated to 0.7 mM and exchanged into 0.1 M sodium phosphate buffer pD 7.0, D_2O/H_2O 90:10 solution. ^{1}H chemical shifts were referred to 3-(trimethylsilyl) 2,2,3,3-tetradeuteropropionic acid sodium salt (TSP-d_4).

Resonance Raman (RR) spectra were recorded on a HoloProbe Raman spectrograph (Kaiser optical systems) coupled to an Olympus BX-60 optical microscope. Excitation was provided by the second harmonic from a Nd^{3+}:YAG laser (Showa Optronics JUNO 532-100S). The laser intensity was 10 mW at the sample surface. The backscattering from the sample in glass capillaries was collected at 20 ˚C with a

thermoelectrically cooled CCD detector through Kaiser super notch filters and optical fibers. The oxidized C-cyt c_z solution contained 83.3 μM of C-cyt c_z in a buffer of 30 mM Tris-HCl (pH8.5) with no further oxidizing agent. The Raman scattering from the reducing agent (1 mM dithiothreitol) was negligible. Each spectrum was obtained from a fresh C-cyt c_z to minimize the laser-induced degradation of the sample, and five spectra from different samples were accumulated.

Crystallization of the Expressed C-cyt c_z. The purified C-cyt c_z was concentrated using Amicon YM-10 and adjusted to 4.5 mM. Crystallization was performed using the sitting-drop vapor-diffusion method at 20 ˚C, each drop consisting of 0.5 μL of protein solution and 0.5 μL of precipitant solution equilibrated against 400 μL of precipitant solution. Very small crystals were obtained in 2.0 M ammonium sulfate and 0.1 M sodium acetate pH 4.6. Initial screening trails were performed using Crystal Screens I, II, Cryo and PEG/Ion (Hampton research). The crystallization conditions were optimized and crystals suitable for X-ray diffraction experiments were obtained using low molecular weight polyethylene glycol (PEG) as an additive. The drop comprising 2 μL of protein solution mixed with the same volume of precipitant solution was equilibrated against 0.4 mL of precipitant solution containing 0.1 M sodium citrate, pH 4.5, 1.4 M ammonium sulfate, 2~4%v/v PEG400.

X-ray Diffraction Experiment. The C-cyt c_z crystals were soaked in a cryoprotectant

solution containing 0.1 M sodium citrate, pH 4.5, 1.4 M ammonium sulfate, 5%v/v PEG400 and 20% glycerol for a few seconds and then flash-cooled at 100 K. X-ray diffraction data were collected at 100 K on an ADSC Quantum 210 detector using synchrotron radiation with a wavelength of 1.0000 Å at the AR-NW12A station of The Photon Factory (KEK Japan). Complete data set was collected from a single crystal. For high-resolution data collection, the crystal-to-detector distance was 80 mm, and the data were collected from 360 frames with a rotation angle of 0.5º and an exposure time of 5 sec/frame. For low-resolution data collection, the crystal-to-detector distance was 200 mm, and the data were collected from 180 frames with a rotation angle of 1º and an exposure time of 0.3 sec/frame. The diffraction data were processed and scaled using the HKL-2000 program package (Otwinowski and Minor, 1997).

Results and Discussion

Expression, Purification and Identification of the C-cyt c_z

The C-cyt c_z was highly expressed in *E. coli* C41 cells in the presence of pEC86 plasmid without using IPTG for induction. The pEC86 plasmid expresses the *ccmABCDEFGH* genes that are needed for heme incorporation in cyt *c* (Arslan et al., 1998). The C-cyt c_z appeared to be expressed in the periplasmic space and can be extracted by osmotic shock. The conventional procedure of protein expression by the IPTG induction failed as the apo-C-cyt c_z accumulated on inclusion bodies, probably due to some traffic jam in exporting

the protein across membrane into the periplasmic space (data not shown). During the purification, we found that the C-cyt c_z did not adsorb on DEAE column up to pH8.5. This may be attributed to the high value of isoelectric point (pI=8.89) calculated from the composition of C-cyt c_z. However, the eluted C-cyt c_z fractions were highly purified with a ratio of $A_{415}/A_{280} \sim 5$. Further purification by gel filtration resulted in high purity ($A_{415}/A_{280} > 6$) verified by electrophoresis (Fig. 1). The SDS-PAGE band was confirmed by heme staining using 3,3'5,5'-tetramethylbenzidine (Thomas et al., 1976). Primary sequence of the expressed C-cyt c_z was determined by MALDI-TOF/MS. The measured molecular mass of 10745 Da indicates that it is composed of the 90 amino acid C-cyt c_z (Ala117 – Phe206) with two residues (Ala-Met) attached at the N-terminus. The midpoint redox potential was measured to be 188 mV (Hirano et al., 2009), in agreement with that of the cyt c_z in native membrane (Okumura et al., 1994). Under the optimized condition, the final yield was determined to be approximately 17 mg per liter of *E. coli* medium.

Spectroscopic Characterization of the E. coli Expressed C-cyt c_z

The absorption spectrum of oxidized C-cyt c_z (Fig. 2, broken line) is typical of low-spin ferric heme with the Soret band at 409.5 nm. Upon reduction, the Soret band shifted to 415 nm with the appearance of α and β bands at 550.5 nm and 522 nm (Fig. 2, solid line), respectively. There is a very weak peak at about 635 nm for both oxidized and reduced forms (Fig.2, inset) due to a porphyrin-to-iron transition observed for high-spin form of cyt *c* (Lanir et al., 1979). A shoulder around 695 nm was also observed for the oxidized C-cyt

c_z arising from axially iron-bound methionine (Senn et al., 1980). The absorption spectra did not change over 10 days of incubation at room temperature.

Figure 3 shows circular dichroism (CD) and magnetic circular dichroism (MCD) spectra of the C-cyt c_z. The CD spectra observed are similar to those of the corresponding oxidized and reduced forms of the cyt *c* from horse heart (Myer, 1968). The CD signals in 300 to 370 nm region are mainly from tryptophan residues (Fee et al., 2000), here the single Trp201 (referred to the full length cyt c_z), whereas the CD signals in 360 to 460 nm region were proposed to arise from protein-induced deformation of the heme ring (Blauer et al., 1993) and from the interaction of the heme ring with polarized groups in its vicinity (Hsu and Woody, 1971). Secondary structures can be evaluated from the CD spectra in the far ultraviolet region, and the α-helix contents were determined to be 46% and 43% for the oxidized and reduced C-cyt c_z (Fig. 3A, inset), respectively. More accurate information on the iron valence and spin state was obtained from the MCD spectra. The reduced C-cyt c_z exhibited a strong derivative shape for the α band, while the oxidized form showed a derivative-shaped band in the Soret region. Overall spectral shapes and the intensity ratio of Soret to α-band all indicate the presence of a low-spin heme for both ferric and ferrous C-cyt c_z (Ookubo et al., 1987).

The temperature-dependence of one-dimensional ^{1}H-NMR spectra in low- and high-field regions is shown in Fig. 4 for the oxidized C-cyt c_z. Several features were observed from these spectra. Resonances *a* and *b* exhibited significantly large paramagnetic shifts compared to those of the closely related Class I ferric cyt *c* (see below),

for which the largest shifts are typically around 30 ~ 35 ppm (Pielak et al., 1996; Shokhirev and Walker, 1998). Striking differences in the linewidth were observed for some resonances, e.g., peaks *a* and *b*, indicating a difference in the dynamic environment between these protons. Many resonances exhibited anti-Curie behavior (Turner, 1993), i.e., the paramagnetic shifts increase with temperature (e.g., peaks *c* and *d*). Because the CD spectrum around 695 nm (data not shown) and the chemical shift pattern in the low-field region are characteristic of *R*-chirality for the axial methionine (Banci et al., 1994; Senn and Wüthrich, 1983; Shokhirev and Walker, 1998), resonances *a, b, c* and *d* may be provisionally assigned to the 18^1, 7^1, 12^1 and 2^1 heme methyl protons, respectively. The chemical shifts of these resonances did not change over pH range of 6 - 8.

Although the C-cyt c_z has no extensive sequence similarity to other cyt *c*, the heme binding site and axial ligands are completely conserved. In addition, some residues beyond the axial methionine fit the consensus for the C-terminal helical region of Class I cyt *c*. For example, a phenylalanine, three residues after the methionine, matches an aromatic residue in the algal cyt c_6 and the sequence IXXWL is approximately the same distance from the methionine as in Class I cyt *c* (Meyer, 1996). If the C-cyt c_z is related to Class I cyt *c*, it has experienced an approximately 15-residues deletion between the heme binding site and the axial methionine relative to other small bacterial cyt *c* (Hirano et al., 2009).

Figure 5 shows RR spectra of (a) oxidized and (b) reduced C-cyt c_z. Upon excitation of a Q-band (α-β region), the Raman scattering from the porphyrin ring was selectively enhanced due to the resonance with the lowest $\pi \rightarrow \pi^*$ transition. The RR bands

in the reduced and oxidized C-cyt c_z spectra were ascribed to porphyrin in-plane vibrational modes based on those reported for cyt *c* (Desbois, 1994; Hu et al., 1993) and the polarized Raman spectra (data not shown). The depolarized (dp) bands at 1638 cm^{-1} (ν_{10}) and 1564 cm^{-1} (ν_{11}) in the oxidized form were largely decreased in their intensities and red-shifted to 1622 cm^{-1} and 1540 cm^{-1}, respectively, in the reduced form. In contrast, the most intense and anomalously polarized (ap) band at 1587 cm^{-1} (ν_{19}) in the oxidized form was little affected in position or intensity upon reduction. The bands ν_{11} and ν_{19} were thought to be RR marker bands for the oxidation and spin states of the heme iron, respectively, and the band ν_{10} was sensitive to both properties (Spiro and Strekas, 1974). In Figure 5, the bands ν_{10} and ν_{11} were largely affected upon reduction of C-cyt c_z in contrast to the pure spin marker band ν_{19}, suggesting that the spin state of C-cyt c_z was not altered by the change of redox states under the present conditions described. The frequencies of ν_{10} and ν_{19} modes were proposed to be inversely proportional to a C_t–N distance between a pyrrole nitrogen and the center of porphyrin ring (Spiro et al., 1979). According to the spin marker correlation, the C_t–N of C-cyt c_z was estimated to be 2.0 Å, in good agreement with those for the planar low-spin hemes (Spaulding et al., 1975). On the other hand, the ν_{11} mode was proposed to be dependent on the nature of the axial ligands for six-coordinated low-spin ferrous heme complexes (Desbois, 1994; Kitagawa et al., 1975; Okumura et al., 1994; Spiro and Burke, 1976). The ν_{11} mode of the ferrous C-cyt c_z appeared at 1540 cm^{-1} which was slightly lower compared with those of other ferrocytochrome *c* (Desbois, 1994). This may be ascribed to the changes in the ligation property of the axial ligands due to the

interaction between iron e_g (d(π)) and porphyrin e_g(π*) orbitals (Kitagawa et al., 1975; Spiro and Burke, 1976) or the difference in the ionization state of the axial ligands (Othman et al., 1994).

Crystallization and X-ray Diffraction of the E. coli Expressed C-cyt c_z

After a wide-ranging search for optimum screening conditions, crystals of the oxidized C-cyt c_z were obtained from the preparation using ammonium sulfate as a precipitant. Figure 6a shows a micrograph of the crystals. Typically, the crystals showed a rhombic shape with clear edges, and the sizes were approximately 0.1 mm × 0.2 mm × 0.2 mm. The crystals diffracted X-rays to a maximum resolution of 1.2 Å (Figure 6b). The crystal belongs to the tetragonal space group of $I4_1$ (or $I4_3$) with unit-cell parameters $a = b = 74.6$ Å, $c = 111.2$ Å. The complete data set was merged at 1.3 Å resolution from low- and high-resolution data sets with a single crystal in order to avoid incomplete data arising from overload at low-resolution diffractions of high-resolution data set. The crystallographic statistics for the diffraction data are listed in Table 1.

In this study, we described the overexpression, spectroscopic characterization and crystallization of the C-cyt c_z from *Chl. tepidum.* In terms of its unique structural arrangement and crucial role in the electron transfer to the RC special pair, an understanding of the molecular mechanism has long been elusive. This work has paved the way for a detailed structural analysis of the electron carrier domain at atomic level, and the results will be given

in an accompanying paper (Hirano et al., 2009).

Acknowledgments-- We thank Dr. L. Thöny-Meyer for providing us with pEC86 and Dr. T. Kohzuma for the MALDI-TOF/MS measurement. This work has been performed under the approval of the Photon Factory Program Advisory Committee (Proposal No. 2007G585), and was supported by grants-in-aid for Scientific Research on Priority Areas "Structures of Biological Macromolecular Assemblies" and by The Kurata Memorial Hitachi Science and Technology Foundation.

REFERENCES

Arslan E, Schulz H, Zufferey R, Künzler P and Thöny-Meyer L (1998) Overproduction of the *Bradyrhizobium japonicum c*-type cytochrome subunits of the cbb_3 oxidase in *Escherichia coli*. Biochem Biophys Res Comm 251: 744-747.

Banci L, Bertini I, Cambria MT, Capozzi F and Dikiy A (1994) ^{1}H one-dimensional and two-dimensional NMR studies of the ferricytochrome *c* 551 from *Rhodocyclus gelatinosus*. Eur J Biochem 219: 663-669.

Blauer G, Screerama N and Woody RW (1993) Optical activity of hemoproteins in the Soret region. Circular dichroism of the heme undecapeptide of cytochrome *c* in aqueous solution. Biochemistry 32: 6674-6679.

Desbois A (1994) Resonance Raman spectroscopy of c-type cytochromes. Biochimie 76: 693-707.

Fee JA, Chen Y, Todaro TR, Bren KL, Patel KM, Hill MG, Gomez-Moran E, Loehr TM, Ai J, Thöny-Meyer L, Williams PA, Stura E, Sridhar V and McRee DE (2000) Integrity of *Thermus thermophilus* cytochrome c_{552} synthesized by *Escherichia coli* expressing the host-specific cytochrome *c* maturation genes, *ccmABCDEFGH*: biological, spectral, and structural characterization of the recombinant protein. Protein Sci 9: 2074-2084.

Feiler U and Hauska G (1995) The reaction center from green sulfur bacteria, in *Anoxygenic Photosynthetic Bacteria*,(Blankenship RE, Madigan MT and Bauer CD eds), pp 665-685. Kluwer Academic Publishers, Dordrecht, The Netherlands.

Hauska G, Schoedle T, Remigy H and Tsiotis G (2001) The reaction center of green sulfur bacteria. Biochim Biophys Acta 1507: 260-277.

Hirano Y, Higuchi M, Oh-oka H, Miki K and Wang Z-Y (2009) Crystal structure of the electron carrier domain of the reaction center cytochrome c_z subunit from green photosynthetic bacterial *Chlorobium tepidum*. to be submitted.

Hsu M-C and Woody RW (1971) The origin of the heme Cotton effects in myoglobin and hemoglobin. J Am Chem Soc 93: 3515-3525.

Hu S, Morris IK, Singh JP, Smith KM and Spiro TG (1993) Complete assignment of cytochrome c resonance Raman spectra via enzymic reconstitution with isotopically labeled hemes. J Am Chem Soc 115: 12446–12458.

Hurt EC and Hauska G (1984) Purification of membrane-bound cytochromes and a photoactive P840 protein complex of the green sulfur bacterium *Chlorobium limicola* f. *thiosulfatophilum*. FEBS Lett 168: 149-154.

Jenney FE, Prince RC and Daldal F (1994) Roles of the soluble cytochrome c_2 and membrane-associated cytochrome c_y of *Rhodobacter capsulatus* in photosynthetic electron transfer. Biochemistry 33: 2496-2502.

Judd RC (2002) SDS-polyacrylamide gel electrophoresis of peptides, in *The Protein Protocols Handbook, 2nd Ed*,(Walker JM ed, pp 73-79. Humana Press, Totowa, New Jersey.

Kitagawa T, Kyogoku Y, Iizuka T, Ikeda-Saito M and Yamanaka T (1975) Resonance Raman scattering from hemoproteins. J Biochem 78: 719-728.

Kusumoto N, Sétif P, Brettel K, Seo D and Sakurai H (1999) Electron transfer kinetics in purified reaction centers from the green sulfur bacterium *Chlorobium tepidum* studied by multiple-flash excitation. Biochemistry 38: 12124-12137.

Lanir A, Yu N-T and Felton RH (1979) Conformational transitions and vibronic couplings in acid ferricytochrome *c*: a resonance Raman study. Biochemistry 18: 1656-1660.

Lee D-W, Öztürk Y, Osyczka A, Cooley JW and Daldal F (2008) Cytochrome bc_1-c_y fusion complexes reveal the distance constraints for functional electron transfer between photosynthesis components. J Biol Chem 283: 13973-13982.

Meyer TE (1996) Evolution and classifcation of *c*-type cytochromes, in *Cytochrome c: A Multidisplinary Approach*,(Scott RA and Mauk AG eds), pp 33-99. University Science Books, Sausalito, California.

Miroux B and Walker JE (1996) Over-production of proteins in *Escherichia coli*: mutant hosts that allow synthesis of some membrane proteins and globular proteins at high levels. J Mol Biol 260: 289-298.

Myer YP (1968) Conformation of cytochromes. J Biol Chem 243: 2115-2122.

Oh-oka H (2007) Type 1 reaction center of photosynthetic heliobacteria. Photochem Photobiol 83: 177-186.

Oh-oka H, Iwaki M and Itoh S (1997) Viscosity dependence of the electron transfer rate from bound cytochrome *c* to P840 in the photosynthetic reaction center of the green sulfur bacterium *Chlorobium tepidum*. Biochemistry 36: 9267-9272.

Oh-oka H, Iwaki M and Itoh S (1998) Membrane -bound cytochrome c_z couples quinol oxidoreductase to the P840 reaction center complex in isolated membranes of the green sulfur bacterium *Chlorobium tepidum.* Biochemistry 37: 12293-12300.

Oh-oka H, Iwaki M and Itoh S (2002) Electron donation from membrane-bound cytochrome *c* to the photosynthetic reaction center in whole cells and isolated membranes of *Heliobacterium gestii*. Photosynth Res 71: 137-147.

Oh-oka H, Kamei S, Matsubara H, Iwaki M and Itoh S (1995) Two molecules of cytochrome *c* function as the electron donors to P840 in the reaction center complex isolated from a green sulfur bacterium, *Chlorobium tepidum*. FEBS Lett 365: 30-34.

Okkels JS, Kjær B, Hansson Ö, Svendsen I, Møller BL and Scheller HV (1992) A membrane-bound monoheme cytochrome c_{551} of a novel type is the immediate electron donor to P840 of the *Chlorobium vibrioforme* photosynthetic reaction center complex. J Biol Chem 267: 21139-21145.

Okumura N, Shimada K and Matsuura K (1994) Photo-oxidation of membrane-bound and soluble cytochrome *c* in the green sulfur bacterium *Chlorobium tepidum*. Photosynth Res 41: 125-134.

Onodera S, Suzuki H, Shimada Y, Kobayashi M, Nozawa T and Wang Z-Y (2007) Overexpression and characterization of the *Rhodobacter sphaeroides* PufX membrane protein in *Escherichia coli*. Photochem Photobiol 83: 139-144.

Ookubo S, Nozawa T and Hatano M (1987) Iron(II) and iron(III) low and high spin complexes formed from *p*-nitrophenolatoiron(III) complex of protoporphyrin-IX-dimethylester in the presence of 1-methylimidazole: magnetic circular dichroism and ^{1}H nuclear magnetic resonance spectroscopic studies. J Inorg Biochem 30: 45-68.

Othman S, Le Lirzin A and Desbois A (1994) Resonance Raman investigation of imidazole and imidazolate complexes of microperoxidase: characterization of the bis(histidine) axial ligation in *c*-type cytochromes. Biochemistry 33: 15437-15448.

Otwinowski Z and Minor W (1997) Processing of X-ray diffraction data collected in oscillation mode, in *Methods in Enzymology Macromolecular crystallography Part A*,(Charles W, Carter J and Robert MS eds), vol 276, pp 307-326. Academic Press, New York.

Pielak GJ, Auld DS, Betz SF, Hilgen-Willis SE and Garcia LL (1996) Nuclear magnetic resonance studies of Class I cytochromes *c*, in *Cytochrome c: A Multidisplinary*

Approach,(Scott RA and Mauk AG eds), pp 203-284. University Science Books, Sausalito, California.

Senn H, Keller RM and Wüthrich K (1980) Different chirarity of the axial methionine in homologous cytochrome c determined by ^{1}H NMR and CD spectroscopy. Biochem Biophys Res Comm 92: 1362-1369.

Senn H and Wüthrich K (1983) Conformation of the axially bound ligands of the heme iron and electronic structure of heme *c* in the cytochromes *c*-551 from *Pseudomonas mendocina* and *Pseudomonas stutzeri* and cytochrome c_2 from *Rhodospirillum rubrum*. Biochim Biophys Acta 746: 48-60.

Shokhirev NV and Walker FA (1998) The effect of axial ligand plane orientation on the contact and pseudocontact shifts of low-spin ferriheme proteins. J Biol Inorg Chem 3: 581-594.

Spaulding LD, Chang CC, Yu N-T and Felton RH (1975) Resonance Raman spectra of metallooctanaethylporphyrins. Structural probe of metal displacement. J Am Chem Soc 97: 2517-2525.

Spiro TG and Burke JM (1976) Protein control of porphyrin conformation. Comparison of resonance Raman spectra of heme proteins with mesoporphyrin IX analogues. J Am Chem Soc 98: 5482-5489.

Spiro TG, Stong JD and Stein P (1979) Porphyrin core expansion and doming in heme proteins. New evidence from resonance Raman spectra of six-coordinate high-spin ion(III) hemes. J Am Chem Soc 101: 2648-2655.

Spiro TG and Strekas TC (1974) Resonance Raman spectra of heme proteins. Effects of oxidation and spin state. J Am Chem Soc 96: 338-345.

Suzuki H, Hirano Y, Kimura Y, Takaichi S, Kobayashi M, Miki K and Wang Z-Y (2007) Purification, characterization and crystallization of the core complex from thermophilic purple sulfur bacterium *Thermochromatium tepidum*. Biochim Biophys Acta 1767: 1057-1063.

Thomas PE, Ryan D and Levin W (1976) An improved staining procedure for the detection of the peroxidase activity of cytochrome *P*-450 on sodium dodecyl sulfate polyacrylamide gels. Anal Biochem 75: 168-176.

Tsukatani Y, Azai C, Kondo T, Itoh S and Oh-oka H (2008) Parallel electron donation pathways to cytochrome c_z in the type I homodimeric photosynthetic reaction center complex of *Chlorobium tepidum*. Biochim Biophys Acta 1777.

Turner DL (1993) Evaluation of ^{13}C and ^{1}H Fermi contact shifts in horse cytochrome *c*. The origin of the anti-Curie effect. Eur J Biochem 211: 563-568.

Table 1.
Data collection statistics. Values in parenthesis correspond to the highest resolution shell.

	high resolution	low resolution	merged (high+low)
Wavelength (Å)	1.0000	1.0000	
Rotation angle (°)	0.5	1	
Exposure time per frame (sec)	5	0.3	
Space group	$I4_1$ or $I4_3$	$I4_1$ or $I4_3$	$I4_1$ or $I4_3$
Unit cell parameters (Å)	$a = b = 74.6$, $c = 111.2$	$a = b = 74.7$, $c = 111.3$	$a = b = 74.6$, $c = 111.2$
Resolution range (Å)	10-1.3 (1.35-1.30)	50-2.0 (2.07-2.00)	50-1.3 (1.32-1.30)
Observed reflections	411476	137921	451143
Unique reflections	71432	20483	73285
R_{sym}, R_{merge} (%)*	5.1 (18.9)	3.3 (9.6)	4.6(20.2)
$I/\sigma(I)$	51.8 (4.9)	61.4 (13.4)	63.5 (4.4)
Completeness (%)	95.9 (95.2)	99.1 (93.9)	98.1 (94.0)

* $R_{sym}/R_{merge} = \sum_{hkl}\sum_i |I_{hkl,i} - \langle I_{hkl}\rangle | / \sum_{hkl}\sum_i I_{hkl,i}$, where $I_{hkl,i}$ is the ith measured diffraction intensity and $\langle I_{hkl}\rangle$ is the average of the intensity.

FIGURE CAPTIONS

Figure 1. Identification of the *E. coli* expressed product by Coomassie brilliant blue stained 20% SDS-PAGE. Right lane: peptide molecular weight marker "DAIICHI". Left lane: C-cyt c_z purified by DEAE and gel-filtration.

Figure 2. Absorption spectra of the purified C-cyt c_z in 30 mM Tris-HCl pH8.5. Solid line: reduced state obtained with 1 mM dithiothreitol. Dashed line: oxidized state. The inset shows an expanded region in 600 – 750 nm.

Figure 3. CD (A) and MCD (B) spectra of the purified C-cyt c_z in 30 mM Tris-HCl pH8.5. Solid line: reduced state obtained with 1 mM dithiothreitol. Dotted line: oxidized state. Inset shows the CD spectra in 200 – 280 nm region.

Figure 4. Extreme downfield and near upfield regions of the 400 MHz ^{1}H-NMR spectra for the oxidized C-cyt c_z at various temperatures. The sample of 0.7 mM was dissolved in 0.1 M sodium phosphate buffer pD 7.0, D_2O/H_2O 90:10 solution.

Figure 5. Q-band resonance Raman spectra of (a) oxidized and (b) reduced C-cyt c_z obtained with 532 nm excitation. The concentration of C-cyt c_z was 83 μM in 30 mM Tris-HCl at pH8.5. The reduced form was kept in 1 mM dithiothreitol.

Figure 6. (a) Typical crystals of the C-cyt c_z with dimension of 0.1 mm × 0.2 mm × 0.2 mm. (b) Diffraction pattern of the C-cyt c_z crystal. The expanded area shows the high-resolution region.

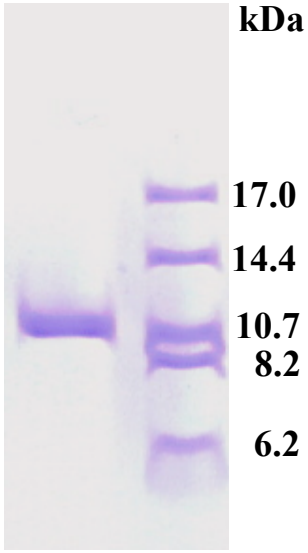

Fig. 1 Higuchi, et al.

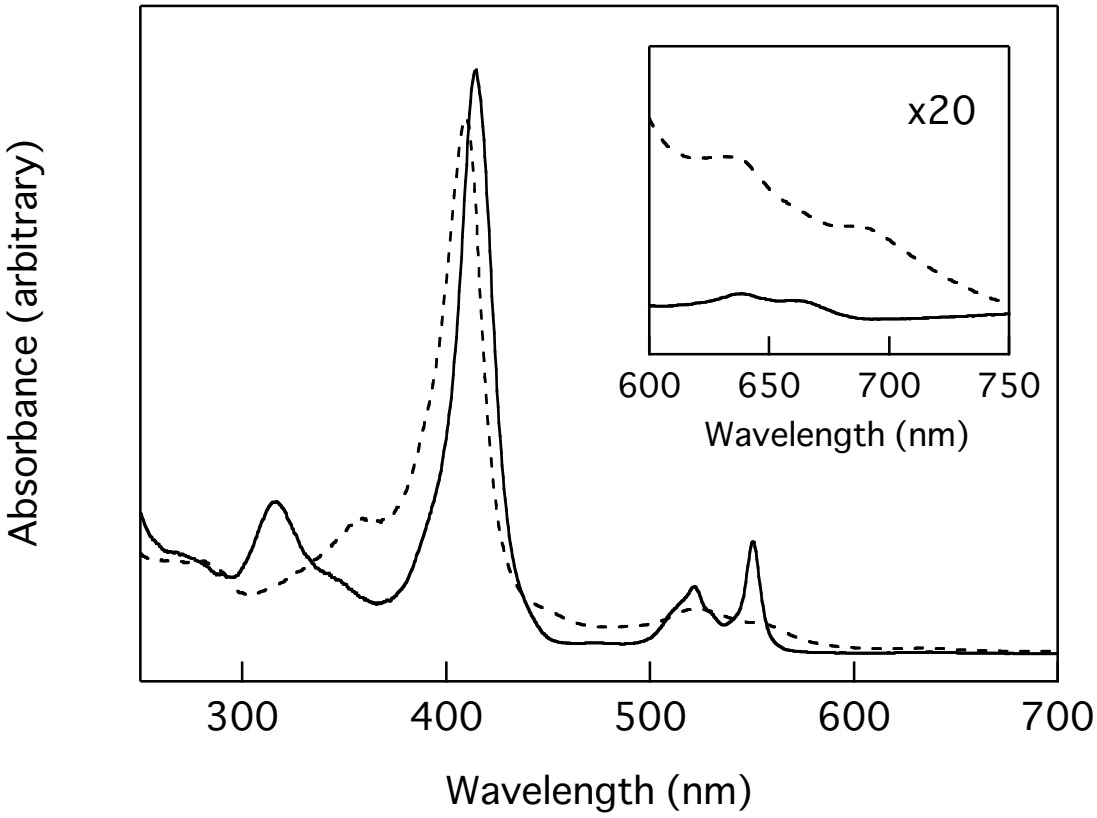

Fig. 2 Higuchi, et al.

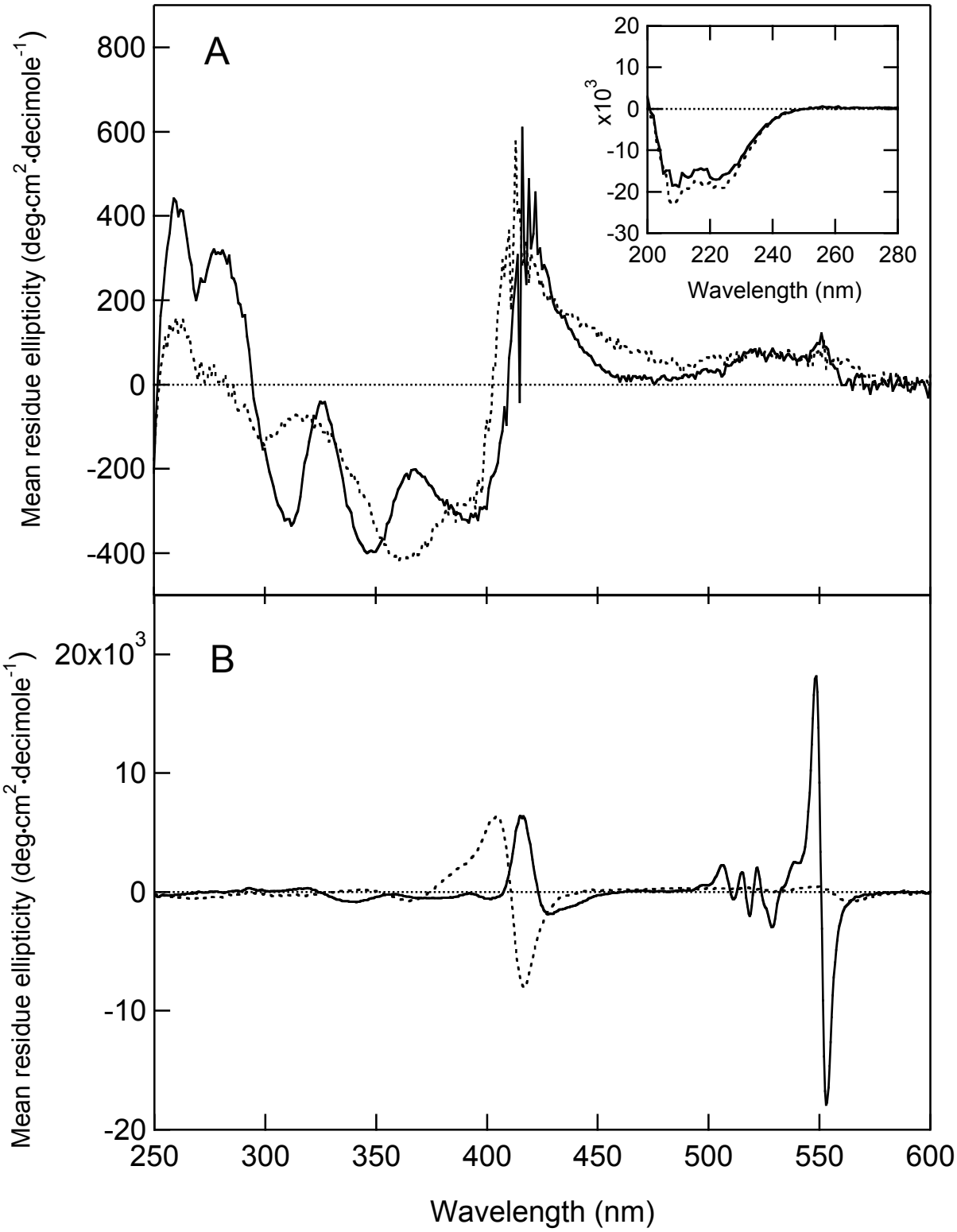

Fig. 3 Higuchi, et al.

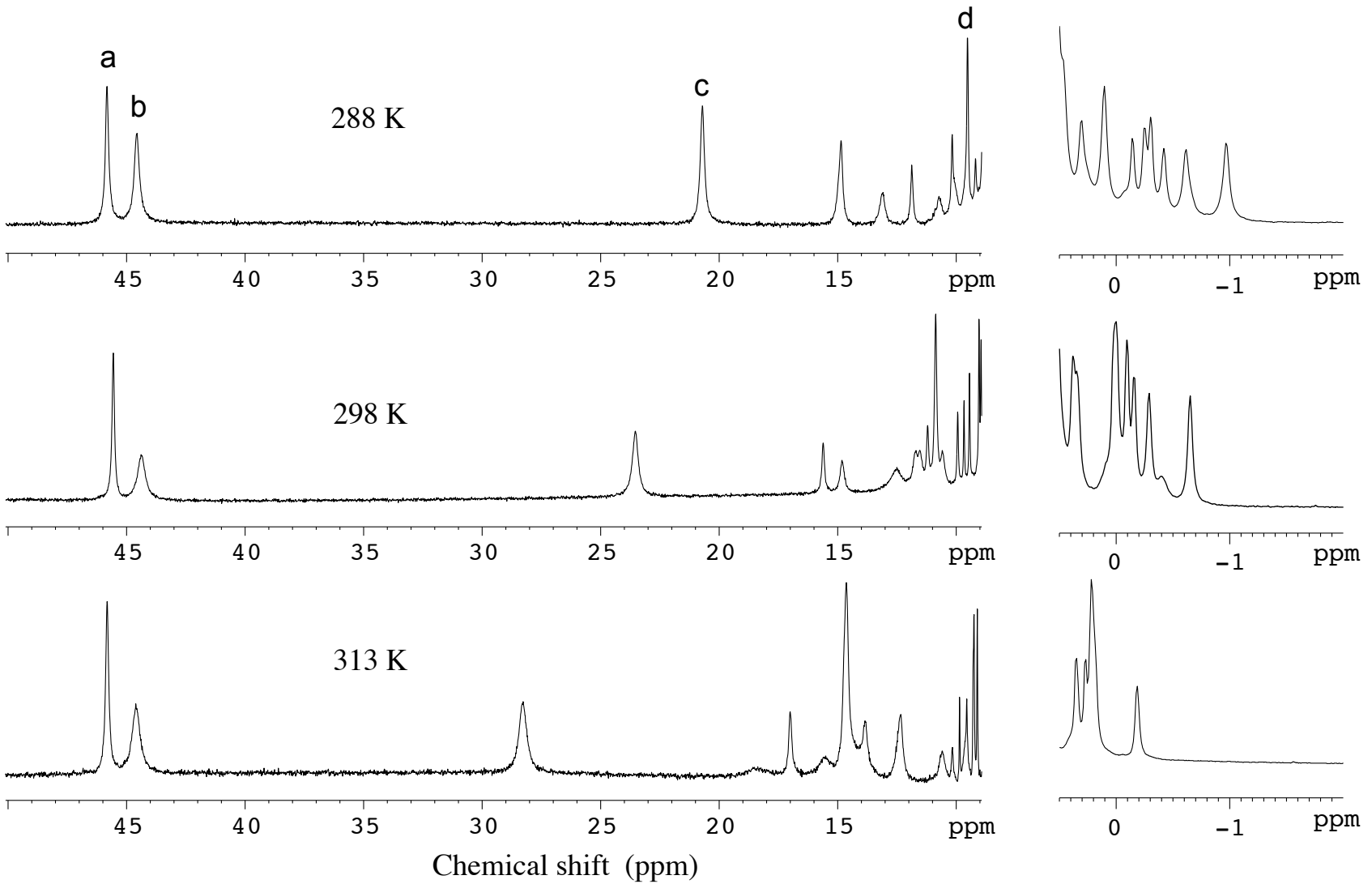

Fig. 4 Higuchi, et al.

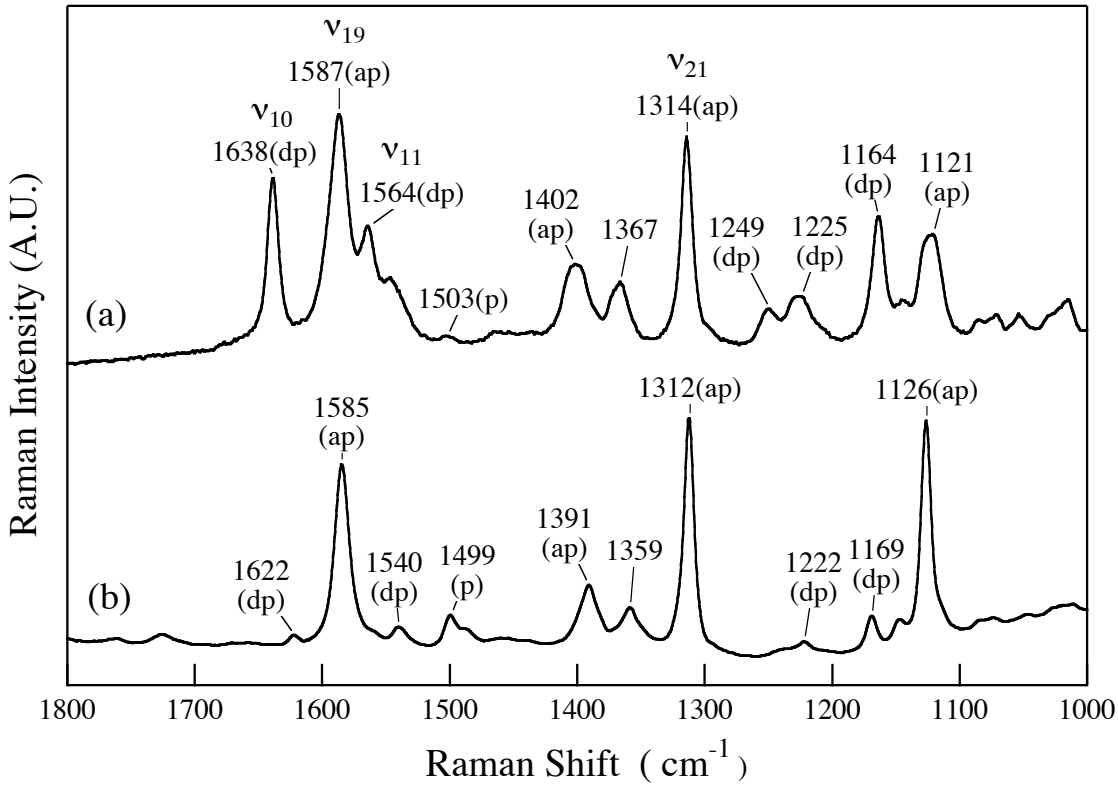

Fig. 5 Higuchi et al.

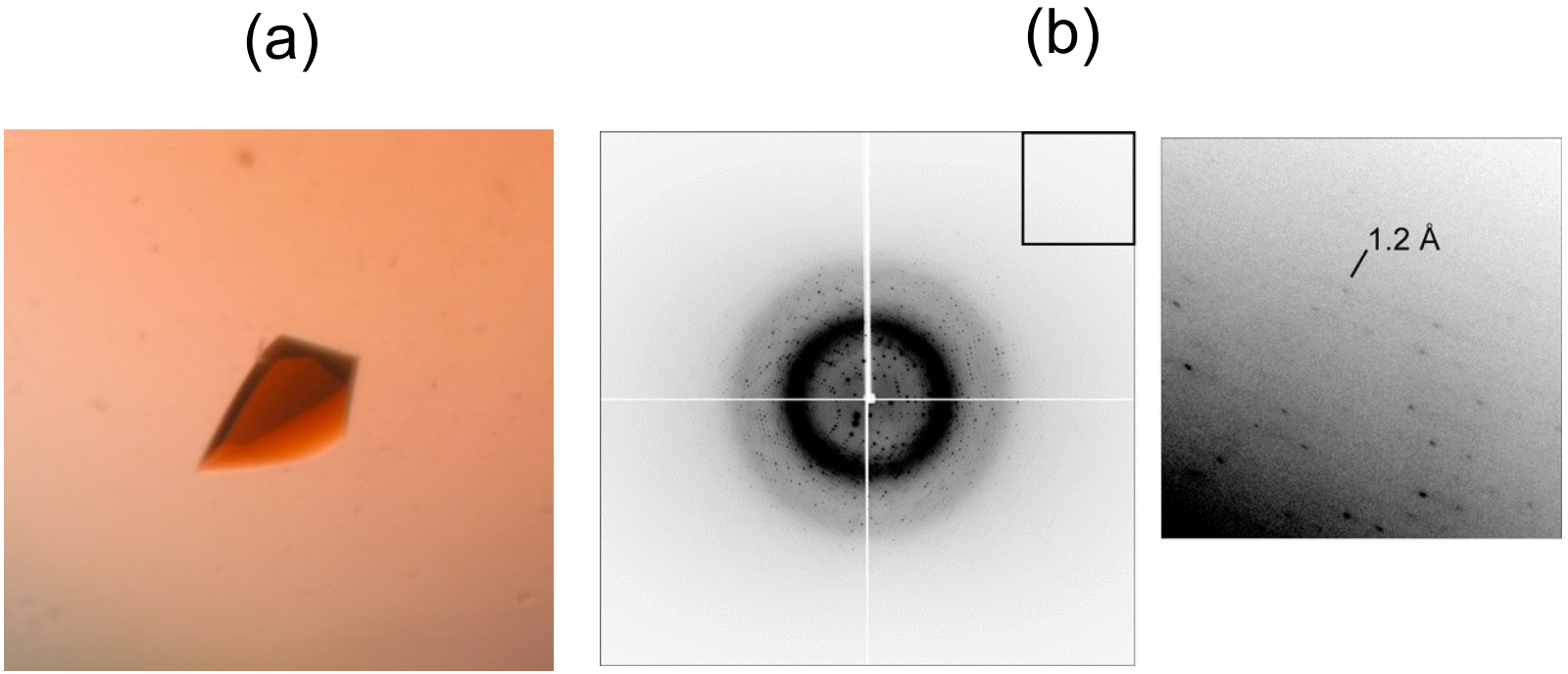

Fig. 6 Higuchi, et al.